Simplified Multi-time Scale Thermal Model Considering Thermal Coupling in IGBT Modules

Zhang, Yi; Wang, Huai; Wang, Zhongxu; Blaabjerg, Frede

Published in:
Proceedings of 2019 IEEE Applied Power Electronics Conference and Exposition (APEC)

DOI (link to publication from Publisher):
10.1109/APEC.2019.8721898

Publication date:
2019

Document Version
Accepted author manuscript, peer reviewed version

Simplified Multi-time Scale Thermal Model Considering Thermal Coupling in IGBT Modules

Yi Zhang, Huai Wang, Zhongxu Wang, and Frede Blaabjerg
Department of Energy Technology, Aalborg University, Denmark

***Abstract*—In the reliability evaluation of power electronic systems, one of the challenges is to model the thermal profiles across multiple time scales, i.e., from switching cycles at nano- or micro-seconds to annual or even longer-time mission profiles. Without consideration of the dissimilarity of thermal behaviors under different time scales, a single thermal model usually leads to either considerable modeling errors or heavy computational burden. Based on the frequency response of thermal impedances, this paper proposes a novel and simplified thermal model to analyze mission profiles with multiple time scales. It enables a computational-efficient thermal stress analysis for power semiconductors, including the thermal coupling in device packages. The theoretical results are verified by experimental testing.**

***Index Terms*—Power semiconductor, reliability, thermal modeling, thermal coupling.**

I. Introduction

The electro-thermal modeling is essential to model-based design and optimization of power electronic converters, especially for the thermal management and reliability analysis [1]–[3]. Temperature is an important stress for the failure of power semiconductor devices according to different industry surveys [4], [5].

As shown in Fig. 1, the mission profiles for reliability evaluation contains from the switching cycles at nano- or micro-second-scale to annual or even longer profiles [6], such as non-periodic profiles at minutes or hours and periodic profiles (i.e., low frequencies, line frequencies, medium frequencies, and switching frequencies). Due to the dissimilarity of thermal behaviors under different time scales, a single thermal model usually is challenging to compromise computational burden with accuracy in the electro-thermal analysis across multiple time scales. The finite element method (FEM) simulation provides delicate and detailed thermal information [7]–[9], but it is difficult to simulate long-term mission profiles due to massive computations. The one-dimensional (1-D) RC lumped models (e.g., Foster, Cauer [10]) are computational light for thermal analysis, but they neglect the thermal cross-coupling in multi-chip modules. In [11], a frequency-domain thermal modeling is proposed to solve the challenges to connect the 1-D Foster models between power devices and heatsinks. Unfortunately, the thermal cross-coupling effect is not included in their study scope. Thermal impedance matrix is a method to model the thermal coupling in power modules [7], [12]. However, the dimension of the thermal matrix is increasing significantly with the number of chips in power modules. In a typical medium power module (e.g., Infineon FF1000R17IE4 with 24 chips), a 24×24 thermal matrix is computational heavy for a long-term mission profile. Moreover, with an increasing request in higher power density and lower parasitics, a more compact power device packaging with multi-chips is one of the trends. It means that the thermal cross-coupling effects are more significant. Therefore, a multi-time simplification method is demanding for long-term mission profile analysis, which takes the accuracy and computational burden into account, and does not ignore the effects of thermal coupling.

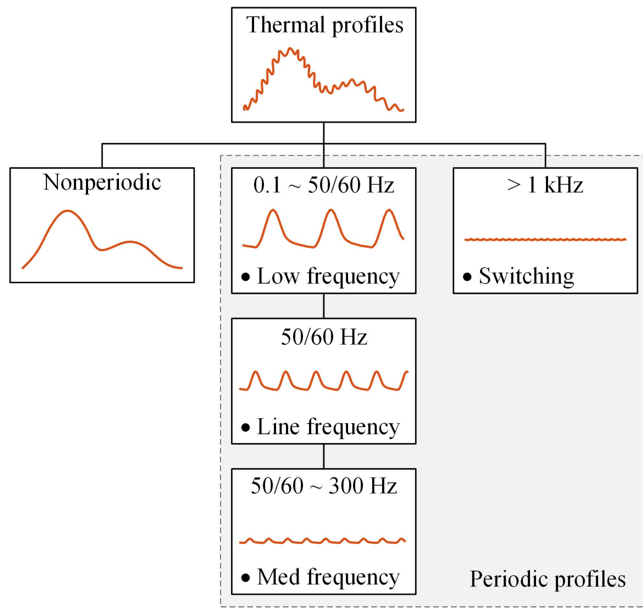

Fig. 1. Typical thermal profiles with different time-scales in power electronic systems.

In order to simplify the thermal analysis in long-term mission profiles, [13] proposed a simplified method for periodic power loss profiles. Moreover, an improved thermal coupling impedance model is proposed in [14], which simplifies the thermal matrix by the chip distance. However, obtaining the boundary chip distance requires FEM simulation and much information of power devices, such as geometrical structures and material properties. In most cases, this information is confidential and difficult to access. Furthermore, [15] simplifies the thermal matrix based on the geometrical symmetries of chips in a power module, but it is limited to the specific packaging types. Consequently, the state-of-the-art raises the requirements for a new simplification method: without needing the confidential information of power devices and unlimited

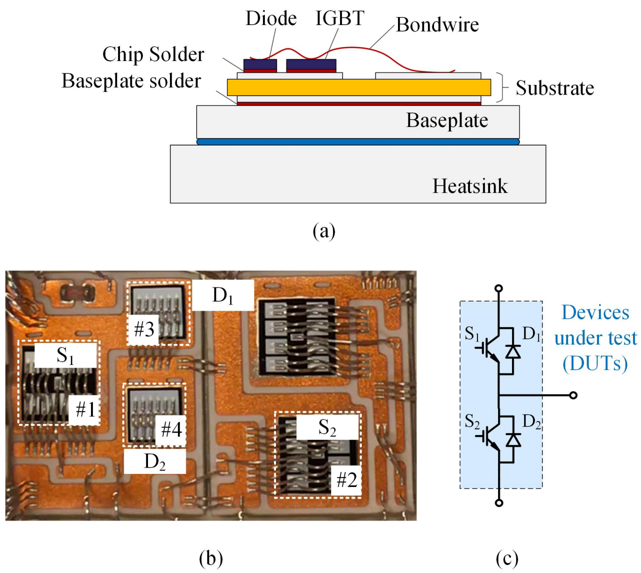

Fig. 2. Studied power semiconductor module: (a) lateral structure; (b) horizontal distribution of chips and (c) circuit diagram.

to any specific packagings.

In this paper, the main contributions are two-fold: 1) the multi-time mission profiles are classified into two types with different frequencies; 2) based on the frequency response of the thermal impedances, a quantitative method is established to simplify the thermal matrix to model the mission profiles with multiple time scales. Experiments verify the corresponding theoretical results at last.

II. Mission Profiles, Thermal Impedance Matrix and Its Challenges

Mission profile based lifetime prediction gains much popularity for reliability analysis in power electronic systems. The modeling from mission profiles into thermal profiles is an essential part for physical-of-failure analysis and further to evaluate the accumulative lifetime consumption of a power device or a power converter. In this section, the compositions of typical thermal profiles and a thermal impedance matrix are introduced. The challenge of considering of the multi-time thermal profiles is also illustrated.

A. The Composition of Typical Thermal Profiles

As shown in Fig. 1, mission profiles in a typical power electronic system consist of multi-time scale composition [16], [17]: 1) Non-periodic profiles: thermal swings due to long-term environmental conditions, typically varying from minutes to hours [18]; 2) Periodic profiles: temperature variations due to periodic power loss profiles, which are classified into four categories. Low frequencies (0.1–50/60 Hz), line frequency (50 Hz), medium frequencies (50/60–300 Hz) and switching frequencies (typically higher than 1 kHz). The purpose of the modeling process is to obtain the multi-time scale thermal profile of IGBT modules from its environmental conditions (i.e., ambient temperature) and power loss profile, in a time-efficient way with sufficient accuracy level. Thus, the discussion of the paper is beginning with the thermal impedance matrix considering thermal cross-coupling inside the IGBT modules.

B. Thermal Impedance Matrix to Estimate the Thermal Behaviors

Considering thermal modeling of a power electronic system, the implementation of the thermal model determines the temperature profiles as consequence of mission profiles. For a single heat source (single chip device), the junction temperature is determined by the power losses from itself only. However, for a multi-chip module, each heat source (silicon chip) contributes to increasing the temperature of itself, also impact on the temperatures of the neighboring chips. Then, the thermal model is defined as a thermal matrix, which is

$$\begin{aligned}
&\begin{bmatrix} T_{j1} \\ T_{j2} \\ \vdots \\ T_{jn} \end{bmatrix} \\
&= \begin{bmatrix} Z_{\text{th},11} & Z_{\text{th},12} & \cdots & Z_{\text{th},1n} \\ Z_{\text{th},21} & Z_{\text{th},22} & \cdots & Z_{\text{th},2n} \\ \vdots & \vdots & \ddots & \vdots \\ Z_{\text{th},n1} & Z_{\text{th},n2} & \cdots & Z_{\text{th},nn} \end{bmatrix} \begin{bmatrix} P_1 \\ P_2 \\ \vdots \\ P_n \end{bmatrix} + T_r \\
&= (\mathbf{Z}_{\text{th,self}} + \mathbf{Z}_{\text{th,mutual}}) \cdot \mathbf{P} + T_r
\end{aligned} \tag{1}$$

where T_j is the junction temperature of each chip, P is the corresponding power losses and T_r is the reference point temperature. The diagonal elements $Z_{\text{th},ii}$ correspond to the self impedances of each chip $\mathbf{Z}_{\text{th,self}}$, whereas off-diagonal elements $Z_{\text{th},ij}$ are mutual impedances $\mathbf{Z}_{\text{th,mutual}}$. It is visible that the number of chips in a power module determines the dimension of the thermal matrix. For a typical medium power module, e.g., Infineon FF1000R17IE4 with 24 chips, the 24×24 thermal matrix is complicated for long-term mission profiles translation. Therefore, a simplification is necessary to consider the multi-time-scale mission profiles, including the effects of thermal coupling in IGBT modules.

III. Simplification of Thermal Matrix by Frequency-Domain Thermal Response

The thermal impedance matrix is good to consider the thermal coupling in the IGBT modules, but the dimension of the matrix is computational-heavy for a device with a large number of chips, especially in a long-term evaluation. In this section, a novel method is proposed to simplify the thermal matrix according to the frequency-domain thermal response. The proposed method helps to obtain the multi-time-scale thermal profile of IGBT modules in a time-efficient way with a sufficient accuracy level.

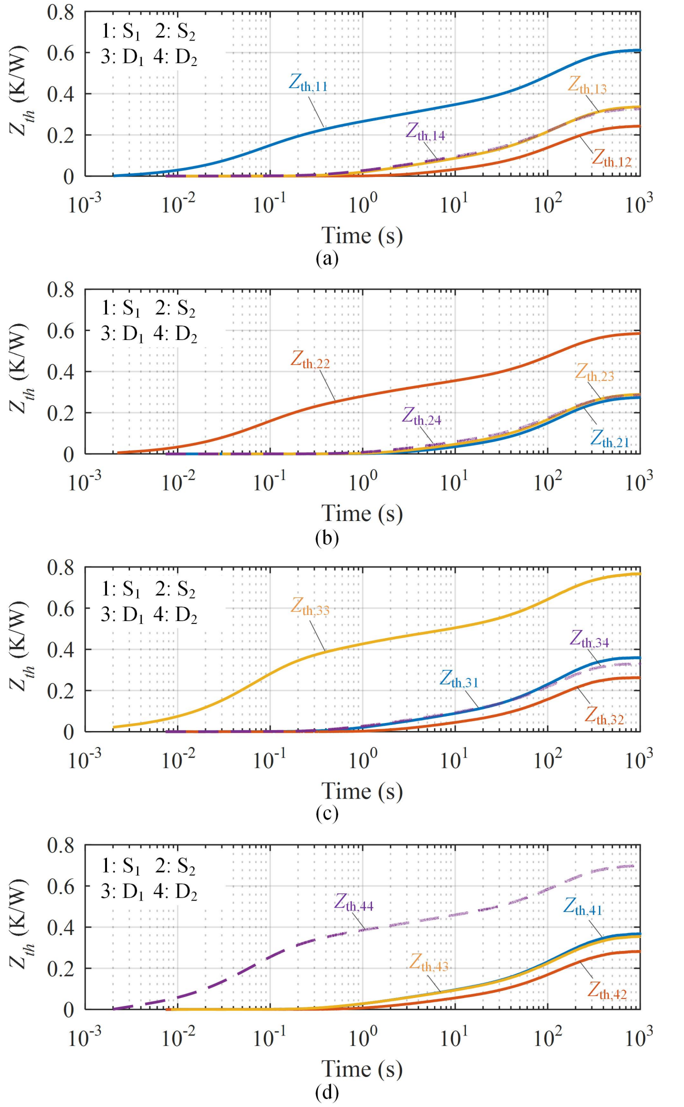

Fig. 3. Measured thermal impedance results to form the thermal matrix of a selected power module.

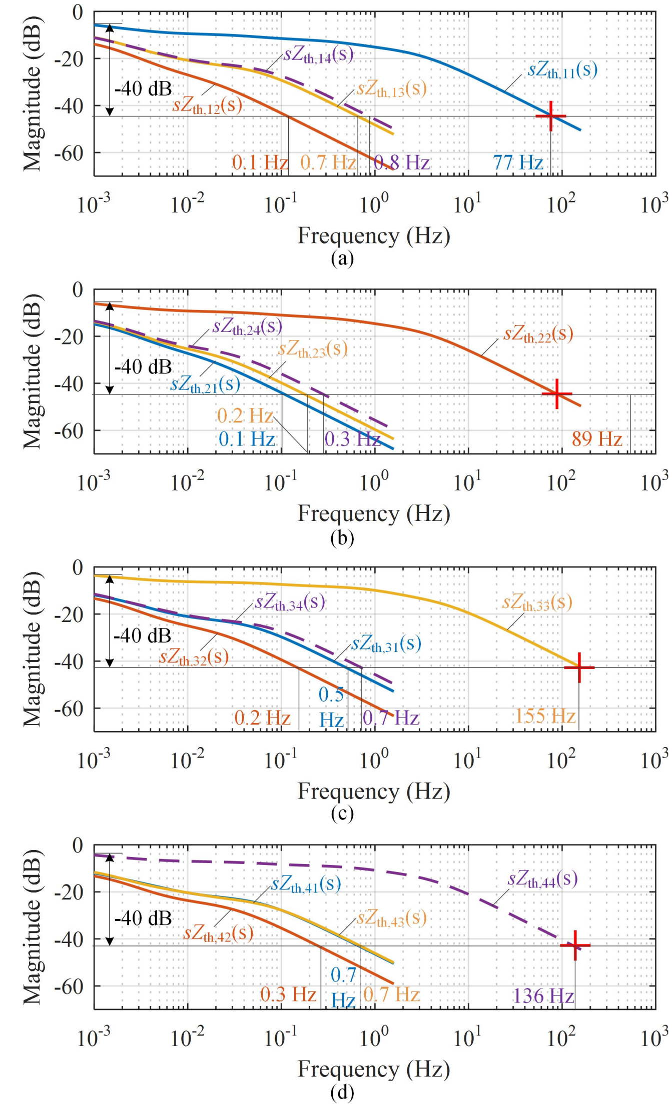

Fig. 5. Frequency-domain response of the thermal impedances in the thermal matrix

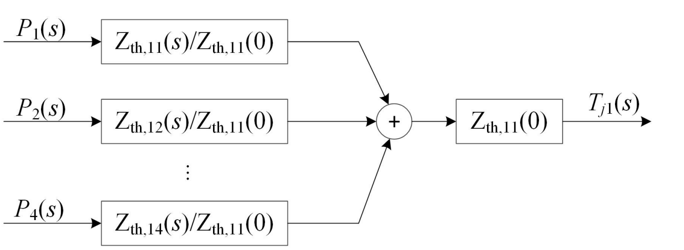

Fig. 4. Block diagram of the modeling of thermal response of T_{j1} in the frequency domain.

A. Selected IGBT Module and Time-Domain Thermal Impedance

Fig. 2 shows an IGBT module F4-50R12KS4 from Infineon, consisting of two IGBT chips and two diodes chips in a half bridge. To form the thermal matrix, a series of experiments is performed by applying square wave power pulses to individual chips to measure the thermal responses. The measured thermal impedance results are shown in Fig. 3, where the measured self-impedances Z_{ii} are always larger than the mutual impedances Z_{ij}. However, it is difficult to find any rules to simplify the thermal matrix based on the time-domain thermal response.

B. Frequency-Domain Thermal Response and Simplification of the Thermal Matrix

Since the relationship between the thermal impedances and frequencies is not obvious in the time domain, the measured thermal impedances are converted into the frequency domain. According to (1), the junction temperature of the first chip is

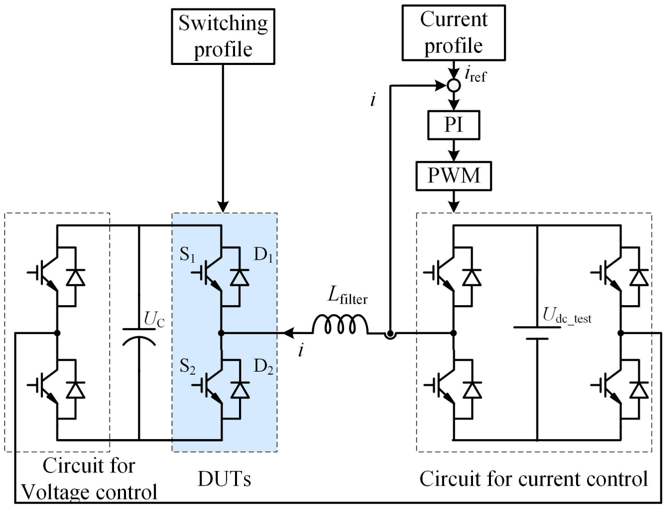

Fig. 6. Experimental circuit configuration, where the circuit for voltage control is adopted to manage the dc-voltage of the DUTs, and the circuit for current control is employed to control the ac current.

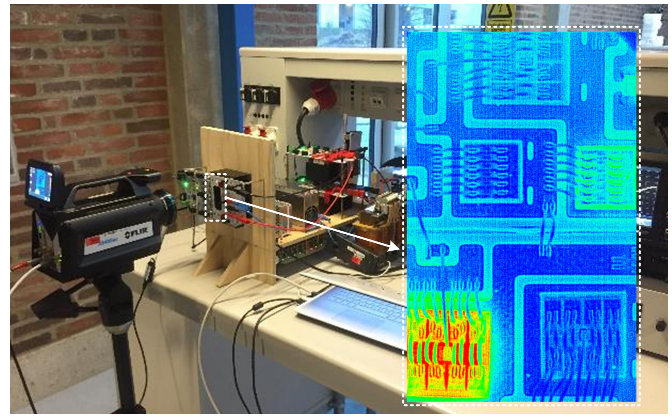

Fig. 7. Experimental platform and the measured thermal distribution by an Infrared camera.

TABLE I
EXPERIMENTAL PARAMETERS.

Parameters	Symbols	Values
IGBT module	S_1, S_2, D_1, D_2	F4-50R12KS4
Power supply voltage	$U_{\text{dc\_test}}$	30 V
DC blocking voltage of the device	U_{c}	300 V
Filter inductance	L_{filter}	3 mH
Switching frequency	f_{sw}	1.5 kHz
Peak value of ac current	$I_{\text{ac\_max}}$	20 A

expressed as

$$T_{j1}(s) = Z_{\text{th},11}(s)\,P_1(s) + Z_{\text{th},12}(s)\,P_2(s) + \cdots + Z_{\text{th},14}(s)\,P_4(s) \tag{2}$$

Moreover, due to the measured self-impedances (e.g., $Z_{\text{th},11}$) are dominant in the thermal responses as shown in Fig. 3, the thermal response in the frequency domain is rewritten by the steady-state value of the self-impedance $Z_{\text{th},11}(0)$, which is given by

$$T_{j1}(s) = Z_{\text{th},11}(0)\left[\frac{Z_{\text{th},11}(s)}{Z_{\text{th},11}(0)}P_1(s) + \frac{Z_{\text{th},12}(s)}{Z_{\text{th},11}(0)}P_2(s) + \cdots + \frac{Z_{\text{th},14}(s)}{Z_{\text{th},11}(0)}P_4(s)\right] \tag{3}$$

Then, a block diagram is plotted according to (3), which is shown in Fig. 4. For each power loss (e.g., $P_1(s)$), if the magnitude of $Z_{\text{th},11}(s)/Z_{\text{th},11}(0)$ is equal to -40 dB at a specific frequency, then the frequency is defined as the corner frequency. In that case, the corresponding output temperature is less than 1 % of the steady-state response of the self-impedance once the frequency is higher than the corner frequency. Thus, the thermal impedance element over the corner frequency is negligible.

The Bode diagrams of the thermal impedances are shown in Fig. 5. For the thermal impedance $Z_{\text{th},11}$, when the frequency $\geq$ 77 Hz, the corresponding thermal response is smaller than 1 % of the steady-state thermal response of the self-impedance. Thus, $Z_{\text{th},11}$ can be regarded as the zero once the frequency larger than 77 Hz. Similarly, the corner frequencies of the mutual impedances $Z_{\text{th},12}$, $Z_{\text{th},13}$ and $Z_{\text{th},14}$ are 0.1 Hz, 0.7 Hz and 0.8 Hz, respectively. For the power device with four chips, when the frequency of power losses at 0.1 Hz, the mutual thermal impedances $Z_{\text{th},12}$ and $Z_{\text{th},21}$ can be neglected according to the Bode diagrams in Fig. 5. The simplified thermal matrix is as shown in Fig. 8. Furthermore, all the mutual thermal impedances are negligible when the frequency of the power loss profile is at 1 Hz. The corresponding simplified thermal matrix is also shown in Fig. 8. As for the power loss profile at the switching frequency of 1 kHz, both the self-impedance and the mutual-impedances can be removed. As a result, the thermal behaviors at the switching frequencies are neglected [6].

IV. EXPERIMENTAL VALIDATIONS

To verify the proposed theory, a platform is built-up as shown in Figs. 6 and 7. The selected IGBT module is the same as in the study case in § III, and the experimental parameters are listed in Table I. An ac current with an amplitude of 20 A is injected into the module. Then, the four power devices S_1, S_2, D_1 and D_2 are heated up separately. A high-speed infrared camera is utilized to measure the junction temperature of the chips.

When the frequency of the power loss profile is 0.1 Hz, the thermal impedance matrix can be simplified without two mutual thermal impedances $Z_{\text{th},12}$ and $Z_{\text{th},21}$. Then, Fig. 8 compares the measured thermal result with the estimated results based on the original thermal matrix and the proposed method. It is evident that the estimated results coincide with each other. Moreover, when the frequency is 1 Hz, all the mutual thermal impedances are negligible according to the proposed method. In this case, the estimated thermal results also agree with the measurement although the mutual thermal impedances are all neglected. Furthermore, when the frequency is 100 Hz, the thermal amplitude is below 0.3 °C, which typically has a negligible impact on the device fatigue. Therefore, the thermal

Simplified Thermal matrix:

$$\overset{@\,0.1\text{ Hz}}{\begin{bmatrix} Z_{th,11} & 0 & Z_{th,13} & Z_{th,14} \\ 0 & Z_{th,22} & Z_{th,23} & Z_{th,24} \\ Z_{th,31} & Z_{th,32} & Z_{th,33} & Z_{th,34} \\ Z_{th,41} & Z_{th,42} & Z_{th,43} & Z_{th,44} \end{bmatrix}} \quad \overset{@\,1\text{ Hz}}{\begin{bmatrix} Z_{th,11} & 0 & 0 & 0 \\ 0 & Z_{th,22} & 0 & 0 \\ 0 & 0 & Z_{th,33} & 0 \\ 0 & 0 & 0 & Z_{th,44} \end{bmatrix}} \quad \overset{@\,100\text{ Hz}}{\begin{bmatrix} Z_{th,11} & 0 & 0 & 0 \\ 0 & Z_{th,22} & 0 & 0 \\ 0 & 0 & Z_{th,33} & 0 \\ 0 & 0 & 0 & Z_{th,44} \end{bmatrix}}$$

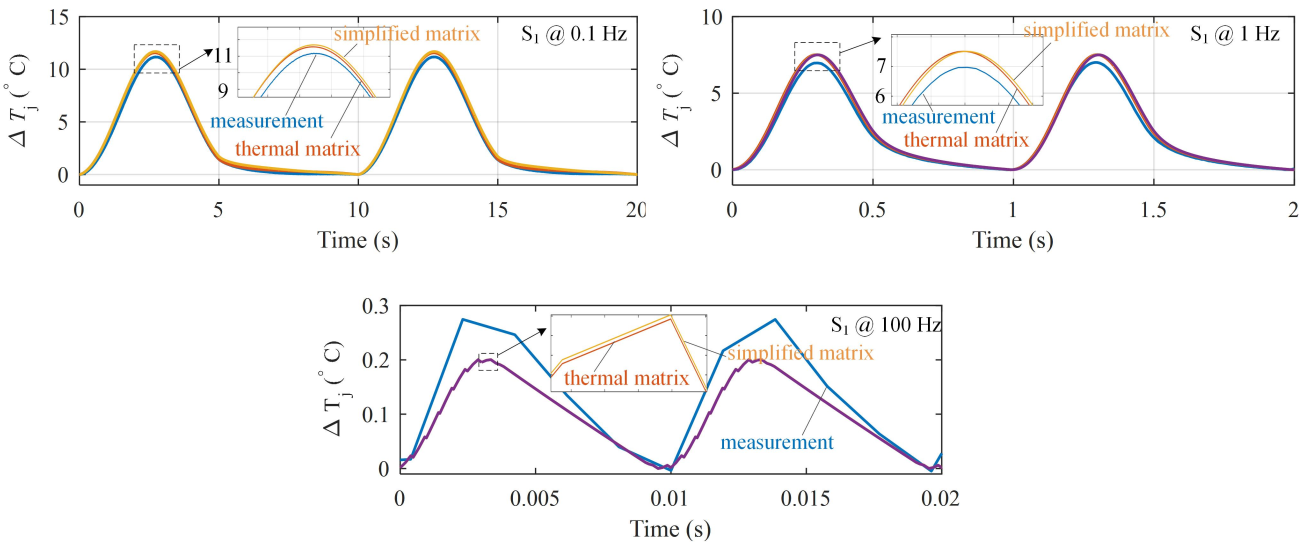

Fig. 8. Simplified thermal matrix and measured thermal results under three different frequencies (0.1 Hz, 1 Hz and 100 Hz).

measurement results support the proposed simplified thermal matrix.

V. Conclusion

In this paper, a simplified thermal model is proposed to reduce the elements of the thermal matrix based on the frequency-domain thermal response. Based on the proposed method, multi-time scale mission profiles can be modeled into thermal profiles by different thermal matrices according to their frequencies. Thus, the computational burden is reduced while the thermal cross-coupling is considered in the method. A 1200 V/50 A IGBT module is selected as a case study, where the time-domain, frequency-domain, and thermal stresses are measured. When the frequency of the power loss profile is low (e.g., 0.1 Hz in the case study), the simplified thermal matrix has many mutual thermal impedances, whereas the mutual thermal impedances can be neglected if the frequency is higher (e.g., $\geq$ 1 Hz in the case study). With further increase of the frequency, the output thermal amplitude is very low, which means even the self-thermal impedances are also negligible (e.g., the switching frequencies).

References

[1] K. Ma, H. Wang, and F. Blaabjerg, "New approaches to reliability assessment - using physics-of-failure for prediction and design in power electronics systems," *IEEE Power Electron. Mag.*, vol. 3, no. 4, pp. 28–41, Dec. 2016.

[2] L. M. Moore and H. N. Post, "Five years of operating experience at a large, utility-scale photovoltaic generating plant," *Progress in Photovoltaics: Research and Applications*, vol. 16, no. 3, pp. 249–259, 2008.

[3] Reliawind, "Project final report on reliability focused research on optimizing wind energy systems design, operation and maintenance: Tools, proof of concepts, guidelines & methodologies for a new generation," Tech. Rep., 2011.

[4] S. Yang, A. Bryant, P. Mawby, D. Xiang, L. Ran, and P. Tavner, "An industry-based survey of reliability in power electronic converters," *IEEE Trans. Ind. Appl.*, vol. 47, no. 3, pp. 1441–1451, Mar. 2011.

[5] ZVEL, "Handbook for robustness validation of automotive electrical/electronic modules," Tech. Rep., Jun. 2008.

[6] H. Wang, M. Liserre, F. Blaabjerg, P. de Place Rimmen, J. B. Jacobsen, T. Kvisgaard, and J. Landkildehus, "Transitioning to physics-of-failure as a reliability driver in power electronics," *IEEE J. Emerg. Sel. Top. Power Electron.*, vol. 2, no. 1, pp. 97–114, Mar. 2014.

[7] A. S. Bahman, K. Ma, P. Ghimire, F. Iannuzzo, and F. Blaabjerg, "A 3-D-lumped thermal network model for long-term load profiles analysis in high-power IGBT Modules," *IEEE J. Emerg. Sel. Top. Power Electron.*, vol. 4, no. 3, pp. 1050–1063, Sep. 2016.

[8] P. D. Judge, M. M. C. Merlin, P. D. Mitcheson, and T. C. Green, "Power loss and thermal characterization of IGBT modules in the Alternate Arm converter," in *Proc. IEEE Energy Convers. Congr. Expo. ECCE*, 2013, pp. 1725–1731.

[9] K. Ma, A. S. Bahman, S. Beczkowski, and F. Blaabjerg, "Complete loss and thermal model of power semiconductors including device rating information," *IEEE Trans. Power Electron.*, vol. 30, no. 5, pp. 2556–2569, May 2015.

[10] A. Wintrich, N. Ulrich, T. Werner, and T. Reimann, *Application Manual Power Semiconductors*. Numremberg, Germany: Semikron Int. GmbH, 2015.

[11] K. Ma, N. He, M. Liserre, and F. Blaabjerg, "Frequency-Domain Thermal Modeling and Characterization of Power Semiconductor Devices," *IEEE Trans. Power Electron.*, vol. 31, no. 10, pp. 7183–7193, Oct. 2016.

[12] T. Poller, S. D'Arco, M. Hernes, and J. Lutz, "Influence of thermal cross-couplings on power cycling lifetime of IGBT power modules," in *Proc.7th Int. Conf. Integr. Power Electron. Syst.*, Nuremberg, Germany, 2012, pp. 1–6.

[13] Y. Zhang, H. Wang, Z. Wang, Y. Yang, and F. Blaabjerg, "Simplified thermal modeling for igbt modules with periodic power loss profiles

in modular multilevel converters," *IEEE Trans. Ind. Electron.*, vol. 66, no. 3, pp. 2323–2332, Mar. 2019.

[14] H. Li, X. Liao, Y. Li, S. Liu, Y. Hu, Z. Zeng, and L. Ran, "Improved thermal couple impedance model and thermal analysis of multi-chip paralleled IGBT module," in *Proc. IEEE Energy Convers. Congr. Expo. ECCE*, 2015, pp. 3748–3753.

[15] Z. Khatir, S. Carubelli, and F. Lecoq, "Real-time computation of thermal constraints in multichip power electronic devices," *IEEE Trans. Components Packag. Technol.*, vol. 27, no. 2, pp. 337–344, Jun. 2004.

[16] P. D. Reigosa, H. Wang, Y. Yang, and F. Blaabjerg, "Prediction of bond wire fatigue of IGBTs in a PV inverter under a long-term operation," *IEEE Trans. Power Electron.*, vol. 31, no. 10, pp. 7171–7182, Dec. 2016.

[17] K. Ma, M. Liserre, F. Blaabjerg, and T. Kerekes, "Thermal loading and lifetime estimation for power device considering mission profiles in wind power converter," *IEEE Trans. Power Electron.*, vol. 30, no. 2, pp. 590–602, Mar. 2015.

[18] Y. Zhang, H. Wang, Z. Wang, Y. Yang, and F. Blaabjerg, "The Impact of Mission Profile Models on the Predicted Lifetime of IGBT Modules in the Modular Multilevel Converter," in *Proc. 43rd Annu. Conf. IEEE Ind. Electron. Soc.(IECON)*, Beijing, 2017, pp. 7980–7985.